



Computational simulation of microneedle penetration in the skin for clinical usage in drug delivery and rejuvenation

Yasaman Amiri, Bahman Vahidi*

Division of Biomedical Engineering, Department of Life Science Engineering, Faculty of New Sciences and Technologies, University of Tehran, Tehran, Iran

ABSTRACT: Microneedles are a type of micron-sized needles that have been considered in recent years in various fields including drug release and rejuvenation. Simulation of penetration process of the microneedle into the skin is useful for examining the strength of the microneedle and its effect on the skin during penetration. In this study, penetration of the microneedles into the skin was simulated using finite element method. The skin is assumed to be in two layers and the Ogden model is applied to each of them. The path of microneedle penetration into the skin is predicted by cohesive elements. The results show that at a constant velocity of 0.36 mm/s in order for penetrating the epidermis only 0.5 s and penetrating the dermis only 2.5 s is needed. By decreasing the tip diameter of the microneedle, the reaction force applied to the microneedle decreased while the maximum stress in the skin also increased. As a result, it is recommended to use a conical model to design the microneedle. When the microneedle speed increases, the reaction force on the microneedle increases exponentially but these changes are more noticeable at high speeds. This simulation can be useful for medical biopsy sampling, drug release systems as well as stress assessment in rejuvenation.

Review History:

Received: May, 27, 2020

Revised: Feb. 06, 2021

Accepted: Feb. 08, 2021

Available Online: Jun. 15, 2021

Keywords:

Microneedle

Skin

Computational Simulation

Finite Element Method

Cohesive element

1- INTRODUCTION

Microneedle is a micron-sized needle that typically has a height of 10–2000 μm and a radius of 10–100 μm and can penetrate directly into the skin through the epidermal layer [1]. Morphologically, microneedles are divided into four types: solid microneedle, coated microneedle, dissolvable microneedle and hollow microneedle [1, 2]. In recent years, microneedles have often been used to provide pharmaceuticals, genes, proteins, RNA, vaccines and diagnostics, and have provided remarkable therapeutic effects [3]. In recent years, drug delivery systems have been rapidly evolving and after oral and intramuscular injection, microneedles has been used as the third most used functional drug delivery system [4, 5]. In addition, not only can the microneedles delivery system increases drug delivery efficiency, but it is also safe and secure and correspondingly improves patient satisfaction [6, 1]. When microneedles enter the skin, they have effects such as pain and inflammation. In this regard, although microneedles have been made in various dimensions and geometries, research to optimize the geometry to reduce pain and inflammation is still ongoing [7]. Due to the high cost of fabricating microneedles, computer simulation of microneedle penetration in the skin can be useful for examining the microneedle's strength and also for its effect on the skin during penetration. Eriketi et al. investigated the penetration depth parameters and buckling

strength by the simulation of three geometries including trilateral, quadrilateral and pentagon. The results showed that microneedle with quadrilateral cross section has the optimum state between two parameters of buckling resistance and penetration depth [4, 8]. Kong et al. investigated the effect of microneedle on the skin and selected the Neo-Hookean model for the skin. In their simulation, the effects of thickness, stiffness and different skin layers were evaluated [9, 10]. Chen et al. developed a nonlinear hyperelastic model for the skin by simultaneously examining the laboratory sample and simulation [11]. It should be noted that during the penetration of the microneedle, the skin is ruptured, so one of the biggest problems of the simulation of skin penetration is the analysis of skin failure model. There have been several models for skin failure so far. One of these models is the element death model [9, 12]. In this method the element is deactivated when the von Mises stress of the elements reaches the failure stress, but this model is more suitable for machining simulations such as drilling [13]. This model also requires programming in subroutine. The ductile material fracture model has also been selected by Maliga et al. [14, 15] to investigate the skin fracture. However, this model does not appear to be appropriate due to different behaviors of the skin and ductile materials. Another model used in this area is the Cohesive model. This is an energy-based approach that predicts the path of failure. Many studies have demonstrated the use of this model to investigate the needle penetration in soft tissues [15,

*Corresponding author's email: bahman.vahidi@ut.ac.ir



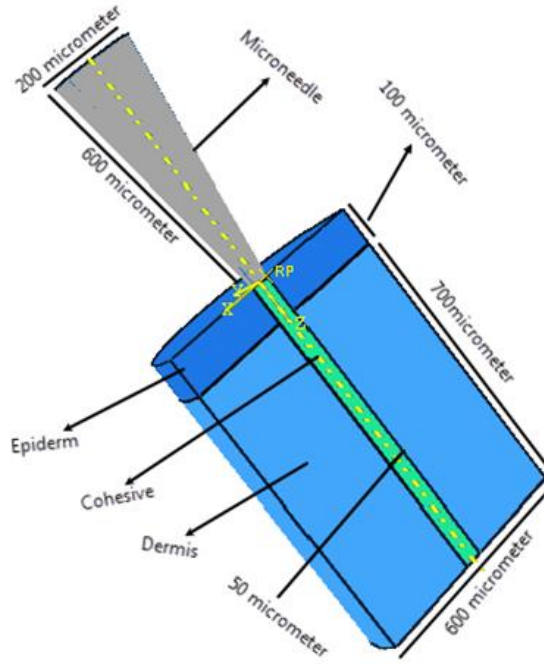


Fig. 1. Dimensions of the microneedle, the skin and the cohesive model.

Table 1. Parameters required for the Ogden model in the human skin [19].

Parameter	α	μ	D
Epiderm	2.9814	4.0991	0
Dermis	3.2876	0.0226	0

16]. In this method, the contact between the needle and the soft tissue is evaluated without the need for elemental death and all the forces required can also be calculated [17]. But in these models, only the penetration of the needle into the simulated gel is investigated and the effect of the micro-sized needle and its geometry on the skin have not been examined. In this study, the penetration of microneedle in the skin was simulated using the Ogden model for human skin and the Cohesive failure model. The reaction force applied to the microneedle, the depth of penetration, and the stress applied to the skin layers during penetration were investigated, and in order for optimizing them, important parameters during penetration such as velocity, the time of penetration and the radius of microneedle's tip were investigated.

2- MATERIALS AND METHODS

2-1- Finite element model for microneedle penetrating in the skin

In this study, a dynamic simulation was accomplished in Abacus 6.14 software with explicit solver. The skin has been considered as a cylinder with a diameter of 600 μm and a height of 800 μm (Fig. 1) with two layers of epidermis and dermis [3]. To reduce the computation and the cost, only half of it is considered and the symmetry condition is defined. Different models such as Neo-Hookean [10] and Ogden [15, 17] have been used to analyze the skin behavior. According to

laboratory data, Ogden is a better model for assessing the skin behavior [18]. The Ogden equation for hyperelastic materials, which is based on the density of strain energy, is expressed as Equation 1 [19]:

$$w(\lambda_1, \lambda_2, \lambda_3) = \sum_{p=1}^N \frac{\mu}{\alpha^2} (\lambda_1^\alpha + \lambda_2^\alpha + \lambda_3^\alpha - 3) \quad (1)$$

Where, α and μ are the constants of the material and λ is the principal stress. The parameters of the Ogden model in Abaqus software for two layers of forearm skin are collected in Table 1. The microneedle is considered as a Conical cylinder with a tip radius of 20 μm and a bottom radius of 100 μm and a height of 600 μm . Microneedle mass is considered to be 1 mg. Contact (surface to surface) was defined between the microneedle surface, the skin and the cohesive surface. Microneedle has a velocity along the skin's height. The distal and the side surfaces of the skin are fixed and have no displacements. The cohesive region is defined as a cylinder with a diameter of 50 μm and a depth of 800 μm in the skin.

2-2- Cohesive method for material failure

For three-dimensional failure simulation, the sum of cohesive plane responses including Mode 1, Mode 2, and Mode 3 is specified. Equation 2 expresses the relationship between these three modes by assuming isotropic shear [20].

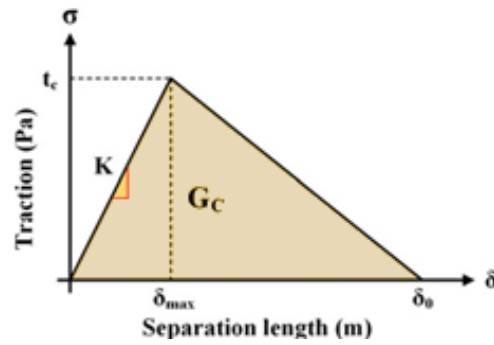


Fig. 2. Traction-separation Diagram [18].

Table 2. Cohesive specifications for the soft tissue [18].

	$G_c(\text{J/m}^2)$	$T_c(\text{MPa})$	$\delta_{max}(\text{mm})$	$\delta_0(\text{mm})$	$K(\text{N/mm}^3)$
Model	37.405	0.7333	0.091	0.102	2.9
Mode 2 and 3	33.664	0.440	0.137	0.153	0.29

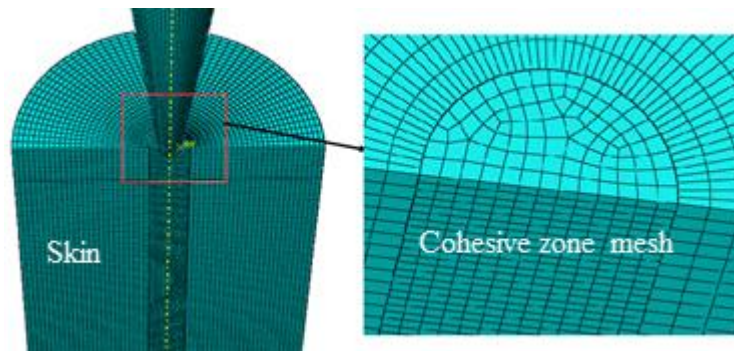


Fig. 3. Mesh of the model in FE.

$$G_1 + (G_2 - G_1) \left(2G_2 / (G_1 + G_2) \right)^\eta = G_C \quad (2)$$

Where G_1 , G_2 and G_3 are equivalent to the fracture toughness. According to the assumption of shear isotropy, $G_2 = G_3$. And the value $\eta = 1$ is set. In each mode, the traction-separation response evaluation is used to determine whether the element is failure or damaged. This relationship is expressed by the critical traction parameter, T_c , the initial and final separation length, δ_{max} and δ_0 , and the initial stiffness, K , and the rate of strain energy released G_c (Fig. 2). The values of cohesive parameters for the soft tissue are given in Table (2).

For the skin, an 8-sided structured mesh is considered. The mesh becomes smaller near the cohesive zone, and as it moves away from the area, the size of the mesh becomes larger. This type of mesh in Abacus is C3D8R and the number of meshes is 110,420. For the cohesive region, the sweep mesh is selected from the cohesive family, which is COH3D8 in Abacus software. For the microneedle, the type of triangle that is R3D3 in Abacus software is finally selected and the number of elements is 26728 (Fig. 3).

2-3- Velocity

According to past laboratory studies[8], microneedle

penetrates the skin, making microneedle a rigid body and penetrating the skin at a constant speed perpendicular to the skin. In this simulation, a constant velocity of 0.36 mm/s was applied to the microneedle penetrating the skin (Fig. 4). However, the initial speed is set to zero, and after 0.1 s it reaches a speed of 0.36 mm/s.

Microneedles enter the skin for various applications and each of these applications need to penetrate a particular depth of the skin. Therefore, it is necessary to determine the depth of penetration with regard to the application of microneedles. For this purpose, a constant velocity of 0.36 mm/s has first been assumed and the applied time has been changed (Fig. 5). If solely the penetration into the epidermis layer is needed, the time should be about 0.5 s and if the penetration to the bottom of dermis is required, it should be about 2.5 s. Changes in the depth of penetration with respect to the velocity change is plotted in Fig. 6. If only the penetration of the epidermis layer is necessary, a velocity of about 0.2 mm/s is required in 2.5 s.

To investigate the effect of the microneedle speed on the reaction force applied to the microneedle, a range of 0.01 to 1 mm/s has been considered. For a better comparison for each of these speeds, a specific simulation time is considered (Table 4). This is while the results are checked at 3 seconds after the

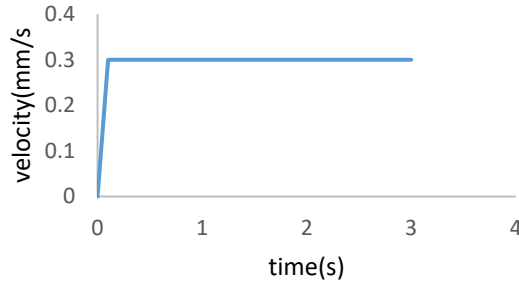


Fig. 4. Changes in the applied speed of the microneedle.

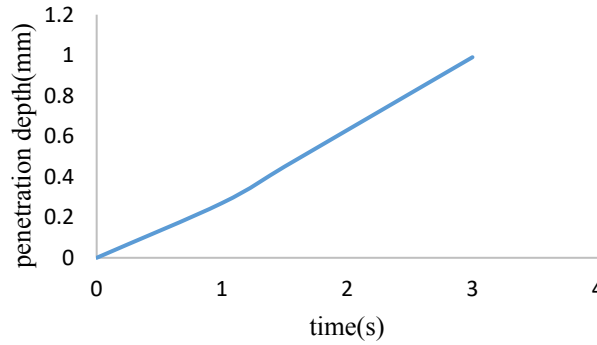


Fig. 5. Investigation of penetration depth at different times in the simulation.

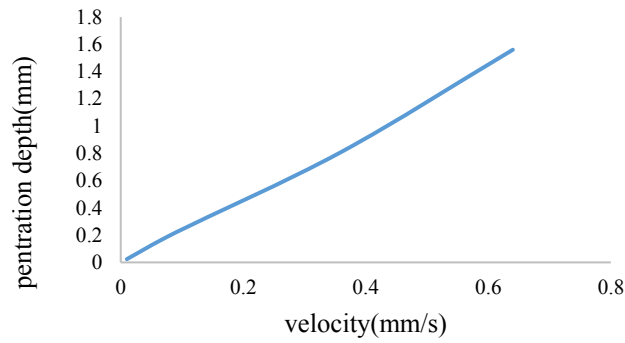


Fig. 6. Investigation of microneedle penetration depth with velocity change.

Table 3. Specifications of speed and time applied to microneedles.

Velocity(mm/s)	0.01	0.04	0.09	0.16	0.25	0.36	1
Time (s)	40	10	6	5	4	3	2

Table 4. Calculation of the maximum stress applied to the skin and the reaction force applied to the microneedle by changing the tip radius.

R _{tip} (μ m)	R _{end} (μ m)	S _{max} in the skin (MPa)	Maximum force reaction (N)
5	100	75	0.06
10	100	74	0.27
20	100	73.3	1.22
22	100	73.3	1.77

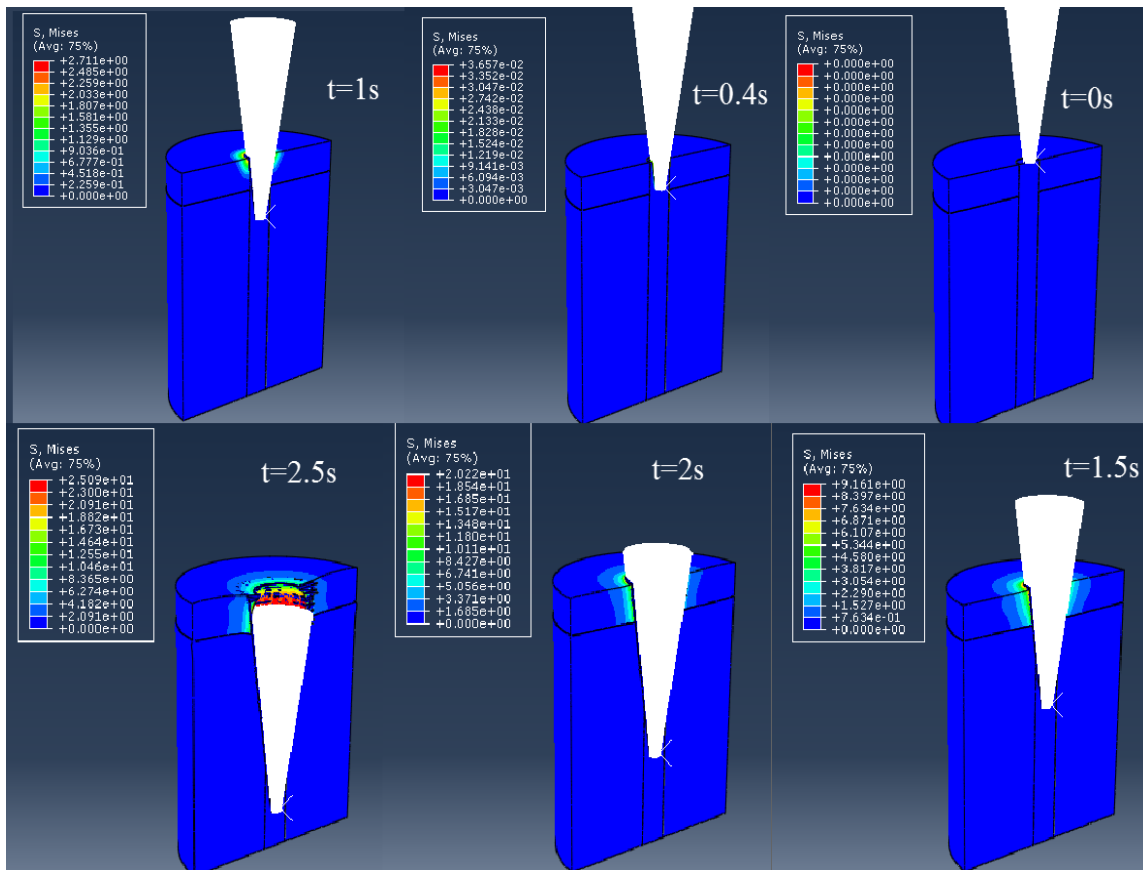


Fig. 7. Stress applied to the skin during the penetration of microneedle.

start of the movement And the previous time is related to the whole process of starting the movement of the microneedle in the skin until it leaves.

3- RESULTS AND DISCUSSION

3-1- Evaluation of the stress applied to the skin

To investigate the results of the simulation, initially von Mises stress applied to the skin at different times from 0 to 2.5 s was examined (Fig.7). The stresses increases as the microneedle enters the cohesive region. This cohesive zone then breaks down and the microneedle gets in contact with other layers of the epidermis. After this step, because the end of the microneedle is wider than its beginning, the stress still increases (up to 2 s) and approximately reaches 60 MPa. After this step, the microneedle enters the dermis layer which has a much lower Young's modulus than the epidermal layer. Therefore, the stress in this layer is much less than in the epidermis. If the microneedle's strength during the penetration is desired, only the epidermis layer can be considered. Due to the fact that the surface of the microneedle is smooth and without bulbs, the distribution of stress in the skin is somewhat homogeneous. Some of the tension created in the skin is due to the penetration of the tip of the microneedle into the skin, while another amount of stress is related to the compressive stress that the end of the microneedle exerts on the skin. Stress from the tip of the needle causes the skin to rupture and may have mechanobiological effects on the skin's

microstructure, including the stimulation of skin collagens. But the stress that the tip of the tiny needle puts on the skin can damage and destroy the skin tissue. The results of the analysis of this section can be useful in evaluating the effect of microneedles on skin rejuvenation and the range of stress required for skin cell growth. Stress in the range of 1 to 10 MPa increases the entry of proteins from the blood vessels into the skin tissue. Given that the stress applied in this study was in the range of 0 to 30 MPa, it can be expected that these microneedles have good performance in this field [21].

3-2- Investigation of microneedle dimensions

The microneedle is designed to be cylindrical with different dimensions at its tip and its end which have a certain angle. In this section, the radius of the end of the microneedle is set to 100 μm and the radius of the tip of the microneedle is variable (Table 5). By varying the radius of the tip of the microneedle from 5 μm to 22 μm , the reaction force and the maximum stress applied to the skin are calculated, which is in agreement with the results of the Kong's study (A linear relationship between surface area and reaction force increase) [10](Fig. 8). It has been observed that as the radius of the tip of the microneedle increases, the reaction force applied to the microneedle increases. Another point to note is that by decreasing the radius of the tip of the microneedle, the reaction force that is applied to the microneedle increases (Fig. 9). Analysis of von Mises stress in the skin shows that as

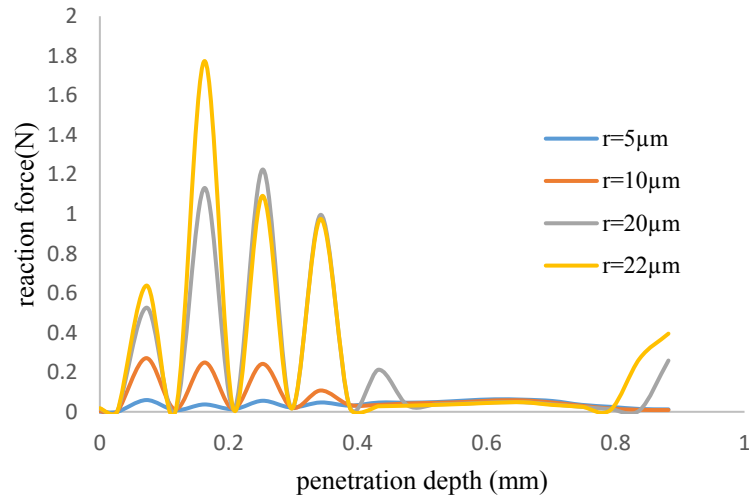


Fig. 8. Diagram of the reaction force applied to the microneedle during penetration at different tip radius of the microneedle.

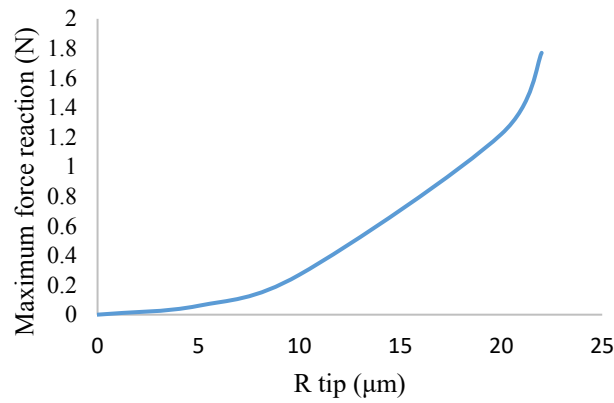


Fig. 9. Maximum reaction force on the microneedle in terms of the needle radius.

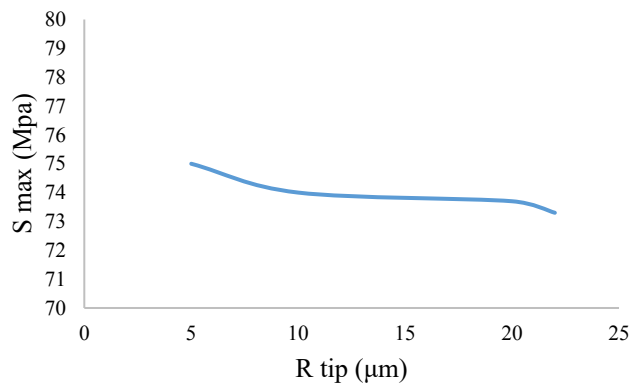


Fig. 10. Maximum stress created on the skin by changing the fine radius of the microneedle.

the tip radius increases, the maximum stress decreases (Fig. 10). However, this reduction in stress is not significant, as only 0.013 MPa has been added to the maximum stress by doubling the radius of the needle tip. However, the maximum force applied to the microneedle is about 4.5 times. The point to be made is that by reducing the radius of the microneedle

tip from 20 μm to 5 μm, the maximum force applied to the microneedle is reduced by about 30 times, and when the radius of the microneedle tip is 5 μm, the reaction force is reduced to 60 mN. This is important for two reasons: first, because of the reaction force applied to the microneedle, which, according to Newton's third law, the same amount of force is applied to

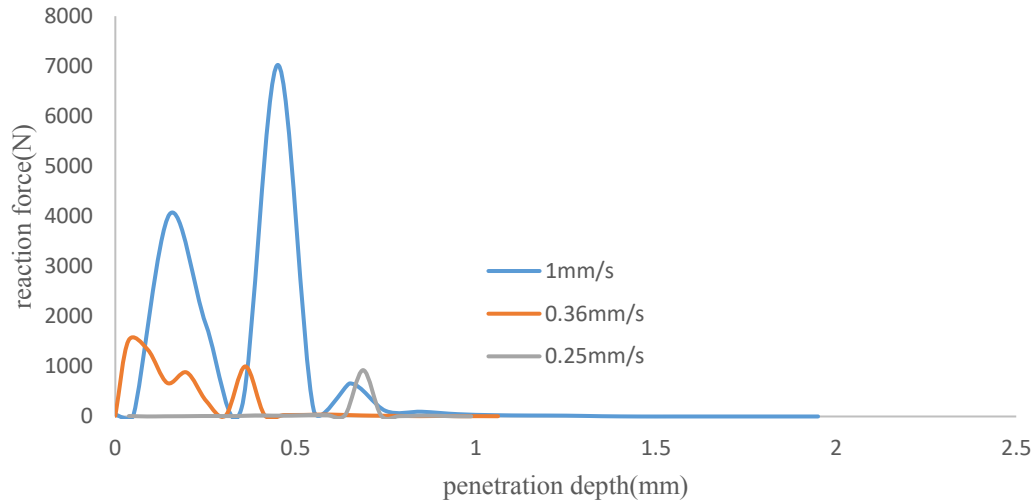


Fig. 11. Changes in the reaction force applied to the microneedle by changing the speed (high speeds).

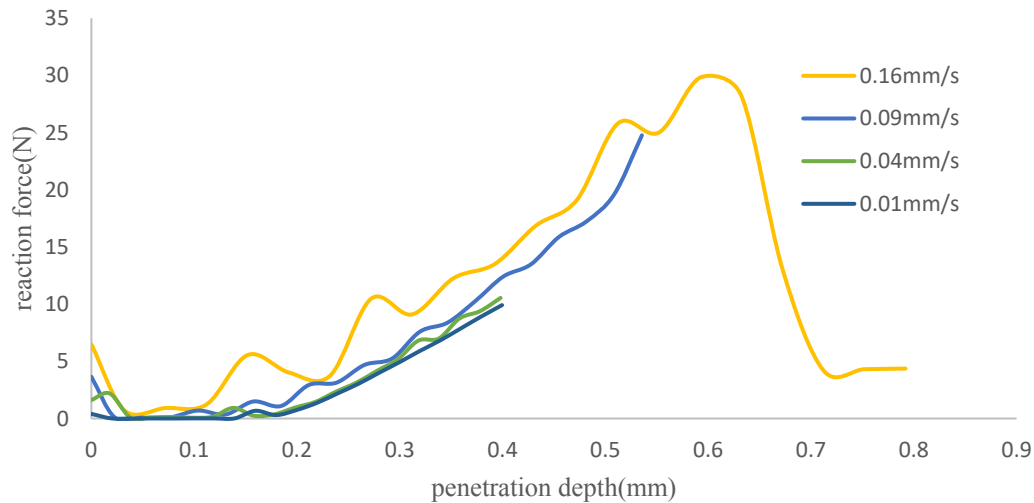


Fig. 12. Changes in the reaction force applied to the microneedle by changing the speed (low speeds).

the skin, and second, because of the force that may cause the microneedle to failure. As a result, it is recommended to use a conical model to design the microneedle. It should be noted that these changes in geometry also affect the strength of the microneedle and when the radius decreases, its strength also decreases. As a result, it should be noted that the microneedle strength is not less than the critical value. Also, the limit of fabrication methods must be considered.

3-3- Investigating the effect of the microneedle speed

In this section, the effect of microneedle speed on the process of penetration into the skin is investigated. According to the proposed cohesive model, the path of skin failure is predicted. Therefore, only the changes in magnitude of velocity have been investigated, and the change in the direction of the microneedle has not been examined, because in this case the general model changes. The results show that when the microneedle's speed increases, the reaction

force applied to the skin increases, so that when the speed reaches 1mm/s, the maximum reaction force applied to the microneedle reaches about 7 N (Fig. 11). At higher speeds, an oscillating state is seen in the amount of reaction force. At low speeds in the initial displacements, a small reaction force is applied to the microneedle, and then the force slowly increases (Fig. 12). Therefore, it should be noted that in the model presented in this study, the microneedle's speed also affects the penetration force.

4- CONCLUSION

Microneedles are nowadays used in drug release, biopsy, and skin rejuvenation systems. Computer simulations can be used to reduce the cost of laboratory tests on microneedles and their harmful effects on the skin. In this study, two layers were considered for the skin and, the Ogden model was used to express the behavior of each layer. The path of failure during the microneedle's penetration was determined by the cohesive elements. The results of this simulation show

that for the penetration into the epidermis layer, only 0.5 s of movement at 0.36 mm/s speed is required. Moreover, to penetrate the dermal layer, this time should be increased to 2.5 s. As the microneedle's tip radius increases, the reaction force applied to the microneedle decreases but the stress on the skin decreases. By reducing the radius of the microneedle's tip to 5 μm , the reaction force applied to the microneedle decreases to 60 mN during penetration. Increasing the speed of the microneedle increases the reaction force on the microneedle exponentially. The results of this simulation can be effective for accurate drug release in the skin as well as stresses applied to the skin. Due to the wide range of geometries used for microneedles, only circular cross-section geometry was used in the present study without adding grooves and barbs to the surface, which could be considered in future researches. In this study, microneedle was considered a rigid body and the stress applied to it was not investigated to determine its fracture strength.

REFERENCES

- [1] Y.-C. Kim, J.-H. Park, and M. R. Prausnitz, "Microneedles for drug and vaccine delivery," *Advanced drug delivery reviews*, vol. 64, no. 14, pp. 1547-1568, 2012.
- [2] H. C. Son, J. H. Rho, K. Y. Chang, D. H. Suh, J. H. Rhue, and K. Y. Song, "Treatment of Various Types of Scar with Multihole Meth od-combination of Fraxel and Microneedle," *프로그램북 (구 초록집)*, vol. 58, no. 1, pp. 143-143, 2006.
- [3] Y. Hao, W. Li, X. Zhou, F. Yang, and Z. Qian, "Microneedles-based transdermal drug delivery systems: a review," *Journal of biomedical nanotechnology*, vol. 13, no. 12, pp. 1581-1597, 2017.
- [4] E. Z. Loizidou, N. T. Inoue, J. Ashton-Barnett, D. A. Barrow, and C. J. Allender, "Evaluation of geometrical effects of microneedles on skin penetration by CT scan and finite element analysis," *European Journal of Pharmaceutics and Biopharmaceutics*, vol. 107, pp. 1-6, 2016.
- [5] M. A. Kendall, Y.-F. Chong, and A. Cock, "The mechanical properties of the skin epidermis in relation to targeted gene and drug delivery," *Biomaterials*, vol. 28, no. 33, pp. 4968-4977, 2007.
- [6] J. C. Birchall, "Microneedle array technology: the time is right but is the science ready?," *Expert review of medical devices*, vol. 3, no. 1, pp. 1-4, 2006.
- [7] Y. C. Kim, J. H. Park, and M. R. Prausnitz, "Microneedles for drug and vaccine delivery," (in eng), *Adv Drug Deliv Rev*, vol. 64, no. 14, pp. 1547-68, Nov 2012.
- [8] S. P. Davis, B. J. Landis, Z. H. Adams, M. G. Allen, and M. R. Prausnitz, "Insertion of microneedles into skin: measurement and prediction of insertion force and needle fracture force," *Journal of biomechanics*, vol. 37, no. 8, pp. 1155-1163, 2004.
- [9] E. Z. Loizidou *et al.*, "Structural characterisation and transdermal delivery studies on sugar microneedles: Experimental and finite element modelling analyses," *European Journal of Pharmaceutics and Biopharmaceutics*, vol. 89, pp. 224-231, 2015.
- [10] X. Kong and C. Wu, "Measurement and prediction of insertion force for the mosquito fascicle penetrating into human skin," *Journal of Bionic Engineering*, vol. 6, no. 2, pp. 143-152, 2009.
- [11] X. Kong, P. Zhou, and C. Wu, "Numerical simulation of microneedles' insertion into skin," *Computer methods in biomechanics and biomedical engineering*, vol. 14, no. 9, pp. 827-835, 2011.
- [12] S. Chen, N. Li, and J. Chen, "Development and experimental verification of a nonlinear hyperelastic model for microneedle-skin interactions," in *2012 IEEE 6th International Conference on Nano/Molecular Medicine and Engineering (NANOMED)*, 2012, pp. 61-65: IEEE.
- [13] J. Ling *et al.*, "Effect of honeybee stinger and its microstructured barbs on insertion and pull force," *Journal of the mechanical behavior of biomedical materials*, vol. 68, pp. 173-179, 2017.
- [14] X. Nan, L. Xie, and W. Zhao, "On the application of 3D finite element modeling for small-diameter hole drilling of AISI 1045 steel," *The International Journal of Advanced Manufacturing Technology*, vol. 84, no. 9-12, pp. 1927-1939, 2016.
- [15] M. L. Crichton *et al.*, "Characterising the material properties at the interface between skin and a skin vaccination microprojection device," *Acta biomaterialia*, vol. 36, pp. 186-194, 2016.
- [16] S. C. Meliga, J. W. Coffey, M. L. Crichton, C. Flaim, M. Veidt, and M. A. Kendall, "The hyperelastic and failure behaviors of skin in relation to the dynamic application of microscopic penetrators in a murine model," *Acta biomaterialia*, vol. 48, pp. 341-356, 2017.
- [17] M. Oldfield, D. Dini, G. Giordano, and F. Rodriguez y Baena, "Detailed finite element modelling of deep needle insertions into a soft tissue phantom using a cohesive approach," *Computer methods in biomechanics and biomedical engineering*, vol. 16, no. 5, pp. 530-543, 2013.
- [18] C.-L. Lin and G.-J. Lan, "A computational approach to investigate optimal cutting speed configurations in rotational needle biopsy cutting soft tissue," *Computer methods in biomechanics and biomedical engineering*, vol. 22, no. 1, pp. 84-93, 2019.
- [19] R. B. Groves, S. Coulman, J. C. Birchall, and S. L. Evans, "Quantifying the mechanical properties of human skin to optimise future microneedle device design," *Computer methods in biomechanics and biomedical engineering*, vol. 15, no. 1, pp. 73-82, 2012.
- [20] R. W. Ogden, "Large deformation isotropic elasticity—on the correlation of theory and experiment for incompressible rubberlike solids," *Proceedings of the Royal Society of London. A. Mathematical and Physical Sciences*, vol. 326, no. 1567, pp. 565-584, 1972.
- [21] M. L. Benzeggagh and M. Kenane, "Measurement of mixed-mode delamination fracture toughness of unidirectional glass/epoxy composites with mixed-mode

bending apparatus,” *Composites science and technology*, vol. 56, no. 4, pp. 439-449, 1996.
[22] J. W. Coffey, S. C. Meliga, S. R. Corrie, and M. A. Kendall, “Dynamic application of microprojection arrays

to skin induces circulating protein extravasation for enhanced biomarker capture and detection,” *Biomaterials*, vol. 84, pp. 130-143, 2016.

HOW TO CITE THIS ARTICLE

Y. Amiri, B. Vahidi, *Computational simulation of microneedle penetration in the skin for clinical usage in drug delivery and rejuvenation*, *AUT J. Model. Simul.*, 53(1) (2021) 13-22.

DOI: [10.22060/miscj.2021.18471.5215](https://doi.org/10.22060/miscj.2021.18471.5215)



